

Journal of Materials Chemistry B

Accepted Manuscript



This is an *Accepted Manuscript*, which has been through the RSC Publishing peer review process and has been accepted for publication.

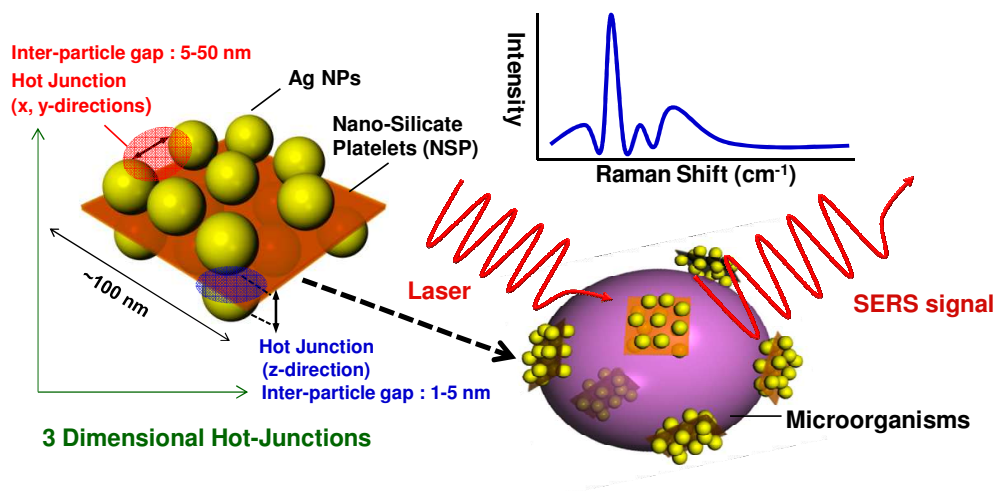
Accepted Manuscripts are published online shortly after acceptance, which is prior to technical editing, formatting and proof reading. This free service from RSC Publishing allows authors to make their results available to the community, in citable form, before publication of the edited article. This *Accepted Manuscript* will be replaced by the edited and formatted *Advance Article* as soon as this is available.

To cite this manuscript please use its permanent Digital Object Identifier (DOI®), which is identical for all formats of publication.

More information about *Accepted Manuscripts* can be found in the [Information for Authors](#).

Please note that technical editing may introduce minor changes to the text and/or graphics contained in the manuscript submitted by the author(s) which may alter content, and that the standard [Terms & Conditions](#) and the [ethical guidelines](#) that apply to the journal are still applicable. In no event shall the RSC be held responsible for any errors or omissions in these *Accepted Manuscript* manuscripts or any consequences arising from the use of any information contained in them.

The table of contents



A novel flexible SERS substrate with 3D hot-junctions capability by employing the nanohybrids of silver nanoparticles and silicate platelets.

Label-Free and Cultured-Free Microbes Detecting by Three Dimensional Hot-Junctions of Flexible Raman-Enhancing Nanohybrid Platelets

Ting-Yu Liu^{1,2*}, Jun-Ying Ho¹, Jiun-Chiou Wei¹, Wei-Chih Cheng³, I-Hui Chen^{4,5}, Jessie Shiue^{4,5}, Huai-Hsien Wang³, Juen-Kai Wang^{3,6}, Yuh-Lin Wang^{3,7} and Jiang-Jen Lin^{1**}

¹Institute of Polymer Science and Engineering, National Taiwan University, Taipei 10617, Taiwan

²Department of Materials Engineering, Ming Chi University of Technology, New Taipei City 24301, Taiwan

³Institute of Atomic and Molecular Sciences, Academia Sinica, Taipei 10617, Taiwan

⁴Research Program on Nanoscience and Nanotechnology, Academia Sinica, Taipei 11529, Taiwan

⁵Institute of Physics, Academia Sinica, Taipei 11529, Taiwan

⁶Center for Condensed Matter Sciences, National Taiwan University, Taipei 10617, Taiwan

⁷Department of Physics, National Taiwan University, Taipei 10617, Taiwan

Corresponding Author(s): T. Y. Liu (*email: tyliu0322@gmail.com) and J. J. Lin (**email: jianglin@ntu.edu.tw)

Abstract

Novel nanohybrid arrays of silver (Ag)-on-silicate platelet with flexibility and three-dimensional (3D) hot-junctions (particularly in z-direction) were discovered for improving the stability of free nanoparticles and the mobility of rigid (glass or silicon-based) substrate in surface-enhanced Raman scattering (SERS) detection technology. Since the Ag nanoparticles are adsorbed on both sides of few nanometer-thick silicate platelets (single-layer exfoliated clay), the geometric arrangement of Ag on both sides of the nanoplatelets (Ag/NSP) may induce strong hot-junctions (z-direction) in reference to the pristine montmorillonite clay (multi-layers) at the thickness of ~20 nm, measured by small molecules (adenine of DNA) and bacteria (*S. aureus*). Enormous red-shifts (16 nm wavelength difference) were observed between single layer and multi-layer silicate platelets, evidenced a huge surface plasmon enhancement comes from hot junctions in z-direction (~7 times higher than 2D hot-junctions of traditional SERS biochip). Further, Ag/NSP SERS substrate displays free floating mobility and optical transparency (less background interference), which inherently increase the contacted surface-area between the

substrate and microorganisms, to enhance the SERS sensitivity. The surface modulation with a surfactant could be complimentary toward a variety of microorganisms including hydrophobic microbes, irregular-shaped microorganisms and larger biological cells due to their mutual specific surface interactions. It was anticipated to apply in the rapid detection for varied microbes with label-free and cultured-free characterizations.

Introduction

Nanohybrid arrays of silver (Ag) nanoparticles /nanoscale silicate platelets (NSP) were synthesized from *in situ* reduction of silver nitrate in the presence of the exfoliated silicate clay and demonstrated a high potency in electronics¹, optical devices², catalysis³, fireproof materials and biomedical applications, such as against bacterial growth⁴⁻⁷ and bio-detection⁸⁻¹⁶ via surface-enhanced Raman spectroscopy (SERS).

In this study we employed the newly developed nanohybrids consisting of silicate platelet supports and the immobilized Ag nanoparticles for SERS detection evaluation. These nanoplatelets were prepared from the exfoliation of the multilayered montmorillonite (MMT) clay with the primary unit structure of lamellar stacks of alumino-silicate platelets and each platelets of two tetrahedral sheets sandwiching an edge-shared octahedral sheet at 2:1 structure at ca. 1.0 nm thickness¹⁷ In literature, most of the studies¹⁸⁻²³ regarding the hybrid materials with Ag nanoparticles were focused on controlling particle sizes, stability and their catalysis properties. The exfoliation of several synthetic and naturally occurring clays including MMT, lucentite SWN and mica to afford NSP nanoplatelets was screened. The NSP from the natural MMT clay with the geometric dimensions of approximately $80 \times 80 \times 1 \text{ nm}^3$ ²⁴⁻²⁵ was found to be most suitable for the bio-detection for SERS due to their high ionic charges on surface, water swelling behavior, and optical transparency and excellent flexibility.

SERS is a recently developed spectroscopic technique based on Raman scattering

enhanced by localized surface plasmon resonance (LSPR) and chemical effects²⁶⁻²⁸. The strong Raman signals from molecules attached to nanometer-sized gold (Au) or silver (Ag) structures. SERS provides the structural information of molecules with high sensitivity and is capable of detecting single molecule non-destructively. Also, this has allowed for extensive chemical and bio-sensing applications including rapid detection of virus and anthrax^{8, 29-30}, sensing of specific DNA³¹, and yeast and cell mapping³²⁻³³. Furthermore, SERS has been employed for label-free sensing of microbes, exploiting its tremendous enhancement in the Raman signal. Recently, a type of SERS-active substrate with uniformly large and highly reproducible Raman-enhancing power has been developed by growing Ag nanoparticles on arrays of anodic aluminum oxide (AAO) nanochannels. Taking the advantage of the sub-10 nm inter-particle gaps in generating 'hot-junctions', an electromagnetic enhancement may be obtained¹³. The high sensitivity and reproducibility of such substrate facilitated the use of SERS for chemical/biological sensing applications.

In order to facilitating SERS for detecting and monitoring of a variety of organisms in environmental and clinical samples, the finding of a flexible SERS could extend the selective detections for the irregular-shaped and large organisms such as fungi and cancer cells. The plate-like clay with double-edged sides of anionic surface charges and a large surface area may serve as the suitable supports for anchoring Ag nanoparticles in generating strong hot-junctions [three-dimensional (3D) hot-junctions]. Furthermore, one-to-few nanometer thickness of NSP in association with Ag nanoparticles can offer excellent flexibility and optic transparency, and consequently the close contact between SERS substrate and microorganisms, resulting in the enhancement of SERS sensitivity. The weakness of the conventional SERS for lacking the affinity toward some bacteria with hydrophobic surface of the cell wall, ca. *E. coli*, and *mycobacteria* could then be overcome. The surface modification by a suitable surfactant, such as polyoxyethylene alkyl ether, ultimately improves the affinity of Ag with bacteria.

Here we report the development of the flexible SERS substrates comprising of silver nanoparticles on nanoscale silicate platelets (Ag/NSP) and optionally modified by a surfactant (Ag/NSS) for advancing the detecting scope of the conventional SERS. Different types of hydrophilic and hydrophobic microorganisms are used to justify the effectiveness of using 3D hot-junctions and flexible nanohybrids.

Results and Discussion

Synthesis of the Ag/NSP nanohybrid

The Ag nanohybrids of Ag nanoparticles supported on nanoscale silicate platelets were synthesized by adopting the exfoliated nanoplatelets from the naturally occurred clays of layered structure. In the presence of the silicate nanoplatelets, the reduction of AgNO_3 in aqueous afforded the nanometer-scale silver particles tethered on platelet surface. The nanoplatelets with the average dimension of 80-100 nm in width and 1-5 nm in thickness provide the large surface-to-weight ratio for stabilizing the *in situ* generated Ag nanoparticles, as shown in Figure 1a. The complex of Ag-on-nanoplatelets had overcome the inherent aggregation of individual Ag nanoparticles through the platelet surface ionic interaction and van-der Waals attraction. It is particularly noted Ag nanoparticles are adsorbed on both sides of NSP surface due to the indiscriminate sandwiching structure of two tetrahedral sheets on edge-shared octahedral sheet in an individual nanoplatelet. Ag nanoparticles separated by few nanometer-thick of silicate platelet spacers (1-5 nm) could create a huge 'hot-junctions' formation and electromagnetic enhancement. Ultimately, it induces strong SERS intensity.

A series of Ag/NSP SERS substrate were prepared by varying Ag/NSP weight ratios from Ag0/NSP100, Ag1/NSP99, Ag7/NSP93, Ag15/NSP85, Ag30/NSP70 to Ag50/NSP50 for evaluating the SERS sensitivity toward bacteria cell walls. The analyses indicated the size of Ag nanoparticles increased from 3.8 nm in Ag1/NSP99 to 35 nm in Ag50/NSP50 in

corresponding to the trend of increasing Ag composition, as shown in Figure 1c-1g and Table S1.

3D hot-junctions and flexibility in Ag/NSP SERS substrate

Many theoretical and experimental works³⁴⁻³⁸ indicated that the precise control of the gaps in the sub-10 nm regime of the nanostructures is critical for the SERS enhancement. However, it is extremely difficult to prepare such a nanostructure and understand the collective surface plasmons existing inside the gaps. In our previous studies¹³, a SERS-active substrate made of an array of Ag nanoparticles partially embedded in AAO with nanochannels was presented. This substrate exhibits an ultrahigh Raman signal enhancement factor due to the controls of the narrow gaps between the Ag nanoparticles. It represents the first quantitative observation of the collective SERS effect on a substrate with precisely controlled ‘hot junction’¹³ by the inter-particle gaps is 5-10 nm regime in the AAO nanochannels. By comparison, the Ag adsorbed on both sides of NSP provides a new aspect of geometric dimension because of the presence of 3D hot-junctions (x-y-z directions of hot junctions), especially in z-direction (the gap of inter-particle distance at 1-5 nm thickness of NSP, as shown in Fig. 2a. TEM image (Fig. 2b) shows silver nanoparticles adsorbed on the both sides of NSP. We suggest that the darker particles are Ag nanoparticles in the top side of NSP, whereas grayer ones are in the bottom side (The evidence shows in Fig. S1). They are separated by exfoliated single layer silicate. Figure 2c indicates that NSP is in a dimension of approximately $\sim 100 \times 100 \times 1 \text{ nm}^3$ observed by the cross section TEM image (sample made by the microtome), and also demonstrates that silver nanoparticles adsorbed on the both sides of NSP.

Moreover, the few nanometer-thick NSP also displays unique flexible and transparent characters. The interaction between Ag/NSP and bacteria was schematically represented and observed by SEM as shown in Fig. 2d-f. It was expected that the Ag/NSP could adhere onto and entangle around the bacteria surface due to its great flexibility. The result shows that

bacteria (*S. aureus*, SA in Fig. 2e and *E. coli*, EC in Fig. 2f) were entangled by thin platelets of Ag/NSP, showing their ultra-flexible or floating behavior and SERS signal could be consequently responded (*ca.* 30 seconds) simultaneously by different platelets with less interference effects due to its high transparency. The response could be differentiated or made it easier in contacting the irregularly shaped microorganisms through rapid surface capturing SERS signal without the uses of other techniques such as labeling and culturing.

Relationship of SERS intensity and inter-particle gap

Figure 3a and Table S1 exhibits the SERS spectra (just z-direction shift) for different Ag/NSP substrate. The SERS signal of bacteria (SA) displays ~30 times enhancement from Ag1/NSP99 to Ag50/NSP50. The optimal Ag30/NSP70 had a higher reproducibility of SERS intensity owing to the narrow particle size distribution, whereas Ag50/NSP50 had reached the maximum SERS intensity but less reproducibility. Moreover, the displays of low and broad continuous background (e.g., Ag30/NSP70 in Fig. 3a) rendering the improvement of signal interference are compared to the previous development of Ag/AAO array substrate¹³ due to their ultra-thin thickness to induce the great optical transparency.

The SERS enhancement appeared to be dependent on the diameter (D) of Ag nanoparticles and their inter-particle gap (W) in x-y direction, as drawn in Fig. 3b. I_{Stokes} (the average Raman signal per Ag nanoparticles) in the exfoliated single platelet substrate increases in opposite to the increase of the inter-particle gap. It is explained that the smaller inter-particle gap in this range generates the corresponding larger hot junctions. In reference to the Ag on MMT, the un-exfoliated MMT with 8-10 layered silicate platelets in each multi-layered stack³⁹ (average thickness: ~20 nm), its I_{Stokes} displays almost half decrease (from 9.3 to 4.3) compared to the similar Ag x-y directional density of Ag/NSP SERS substrate (Ag15/NSP85, single layer stack) due to same degree of increase in their inter-particle gap in z-direction (from ~1 nm to ~20 nm) (Fig. 3b and Table S1). Similar trend was found in the

small molecules SERS detection, such as “adenine” from DNA (Table S2 and Figure 4). The SERS spectra in the bacteria (Fig. 3a) are very similar with adenine (Fig. 4a). We suggest the SERS signal from bacteria might be derived from adenine (DNA) or similar chemical structure compounds released from bacteria.

It is consistent for the factor of the hot junctions in z-direction. In addition, the hot-junction effect would show up in the change of the absorption spectra (UV-Vis spectroscopy), when the W/D is varied. In principle, there should be at least one absorption peak around 400 nm caused by the plasmon resonance of isolated Ag nanoparticles in water. The existence of a red shift in this plasmon peak is another evidence for the hot-junction effect. The result shows that the smaller the value of W/D the wider the red-shifting, as shown in Figure S2. In particular, it displays significant red-shift (16 nm wavelength difference) between single-layered platelet (Ag/NSP, inter-particle gap in z-direction (W_z): 1-5 nm, 411 nm) and multi-layered silicates (Ag/MMT, W_z : ~20 nm, 395 nm), while showing the corresponding SERS enhancement correlated to the hot-junctions in z-direction (Fig. 5). Such an observation could be then named as the effect of 3D hot-junctions.

The inset in Fig. 3b demonstrated the normalized SERS intensity ($I_{\text{Stokes}}/I_{\text{Stokes}}^{\infty}$ ratio) as a function of the W/D ratio for different Ag/NSP substrates. By defining $I_{\text{Stokes}}^{\infty}$ as the SERS intensity for the highest inter-particle gap of Ag1/NSP 99 at ~50 nm, we derived that the ratio of $I_{\text{Stokes}}/I_{\text{Stokes}}^{\infty}$ of the Ag/NSP SERS substrate (single layer) is much higher than that of the Ag/MMT SERS substrate (multi-layers). For example, $I_{\text{Stokes}}/I_{\text{Stokes}}^{\infty}$ ratio equals to 4.7 with W/D=1.9 in Ag15/NSP85 in comparison to the ratio at 2.2 in the Ag/ MMT SERS substrate with W/D=1.4, indicating about few times enhancement, as shown in Fig. 3b and Table S1.

Furthermore, we found the $I_{\text{Stokes}}/I_{\text{Stokes}}^{\infty}$ ratio in 3D hot-junctions of Ag/NSP SERS substrate is much higher than that in the traditional 2D hot-junctions of SERS substrate and literature^{13, 34-38}. For example, $I_{\text{Stokes}}/I_{\text{Stokes}}^{\infty}$ ratio is about 7.1 while W/D is 0.5 in Ag30/NSP70

(Fig. 3b), whereas $I_{\text{Stokes}}/I_{\text{Stokes}}^{\infty}$ ratio is ~ 1 in 2D hot-junctions of the traditional SERS substrate ($W/D=0.5$). It shows 7 times difference of $I_{\text{Stokes}}/I_{\text{Stokes}}^{\infty}$ ratio between 3D and 2D hot-junctions. From above observation, it is deduced that a series of Ag/NSP SERS substrate indeed produce enormous electromagnetic effects to induce huge hot-junctions (x - y - z direction hot-junctions) and thus generate the large SERS enhancement. SERS measurement of the small molecule (adenine) exhibits similar conditions with that of the bacteria, as show in Fig. 4b and Table S2.

Differentiation of SERS signals between hydrophilic and hydrophobic bacteria

We also found the intensity of SERS signal was weaker for detecting hydrophobic bacteria (EC) than for hydrophilic ones (SA), as shown in Figure 6. Two different bacteria were selected for this investigation. The outer membrane of ECs is comprised of lipopolysaccharide and protein as the hydrophobic moieties on the surface, which may mitigate the interaction with Ag/NSP of ionic polarity. With the addition of a surfactant such as the alkyl alcohol ethoxylates (Ag/NSS) could largely alter the surface affinity of Ag/NSP (conceptually illustrated in Fig. 1a and 1b and evidenced by the change of Zeta potentials, not shown here). The example of the hydrophobic bacterium (EC) contrasted the effect of hydrophobic/hydrophilic surface affinity. As a result, the SERS signals ($\sim 730 \text{ cm}^{-1}$) of EC/SA ratio changed from 0.07 by Ag/NSP to 0.9 by Ag/NSS, an increase of 13 times in SERS intensity. The SERS enhancement gave rise to the principle of surfactant-modified SERS substrates that differentiated the bacterial species through characteristics and enhancement of the SERS signal intensity.

Methods and Materials

Synthesis of Ag/NSP SERS substrate

The NSP nanoplatelets (2.0 wt% in de-ionized water) were dispersed by mechanical stirring and added ethanol as the weak reducing agent (Fig. 1a). The NSP dispersion was added with AgNO_3 solution (1.0 wt% in water) at the designated ratio of Ag^+ to NSP. The solution was then stirred for another hour. The process involved the replacement of Ag^+ with Na^+ counter ions on the NSP clay surface and, consequently, reducing the Ag^+ by ethanol in a flask. The mixtures were heated to 80°C for 3 h and monitored by UV-Vis spectroscopy for the color change from yellow to deep-red and the completion of Ag^+ reduction to Ag^0 .

In the example of Ag/NSP at 7/93 weight ratio, NSP solution (9.36 g, 9.94 wt% in water) were dispersed in deionized water to reach a final concentration of 2 wt%, followed by the addition of ethanol (50 ml). The NSP in the co-solvent of water and ethanol was mechanically stirred for half an hour. Then, AgNO_3 (0.11 g) was dissolved in water and added. The Ag/NSP solutions were filtrated and re-dissolved in water to remove the impurities. The preparation of 2D hot-junction (Ag/MMT) SERS substrate is similar with the 3D hot-junction (Ag/NSP) one. It just replaces NSP by MMT. The UV absorption at ~ 400 nm of the final solution indicated the formation of Ag nanoparticles. The inter-particle gaps (W) and the particle sizes (D) were measured by transmission electron microscope (TEM, JOEL JEM-1230) and calculated statistically from an average of at least 100 individual particles with the commercial software (Scanning Probe Image Processor, SPIP™). The stability (UV/Vis) tests of Ag₃₀/NSP₇₀ for 4 hours and the heating stability tests at 80°C for 8 hours were observed in Fig. S3a and Fig. S3b, respectively. These results exhibit strong binding between Ag nanoparticles and NSP, because no significant change of UV/Vis absorption peak.

Synthesis of Ag/NSS SERS substrate

The procedures for preparing the Ag/NSS nanohybrids are described in the followings (Fig. 1b). The NSP dispersion in water was added with SINOPOL 1830 surfactant and abbreviated as NSS. An aliquot of 1 wt % NSP in water suspension (25 g) was added to 1 wt % SINOPOL

1830 in water suspension (25g) in a round-bottomed flask equipped with mechanically stirrer for 30 min at room temperature. The NSS solution (50 g, 1 wt% in water) was added with AgNO₃ solution (5.9 g, 1 wt % in water) and followed by the procedures mentioned above.

Bacteria growth and sample preparation

Staphylococcus aureus (*S. aureus*, SA) and *Escherichia coli* (*E. coli*, EC) purchased from Bioresouce Collection and Research Center in Taiwan. Both bacteria were cultivated for 16 hr. at 37°C on Nutrient and MRS agar base, respectively. After sub-culturing, single colonies were collected using sterile plastic inoculating loops. Bacteria were then suspended in 5 ml of Nutrient and MRS broth respectively, grown for an additional 14 h and then sub-cultured until OD₆₀₀ reached approximately 0.5. Bacteria thus obtained were used for all the experiments. For SERS detection, bacteria were washed and centrifuged three times with deionized water and re-suspended in water again. Typically, the sample solution (1.0 ml) was placed on a SERS substrate and then stored in an orbital shaking incubator (OSI500R, TKS) operated at 120 rpm and 37°C for 1 hr. The sample was washed five times with water before the Raman performance. The detection limits of bacteria/Ag-NSP ratios should be set in the range of 1 to 30 (one unit of bacteria=10⁸ cfu/ml; one unit of Ag-NSP=100 ppm), as shown in Figure 4.

Characterization

Raman measurements were performed with a commercial Raman microscope (HR800, Horiba). He-Ne laser emitting at 632.8 nm served as the excitation source. The laser beam was focused onto the sample through a 50x objective lens. The backward radiation was collected by the same lens and was then delivered to an 80-cm spectrograph equipped with a liquid-nitrogen cooled charge-coupled device for spectral analysis. Raman spectra were collected in the frequency ranging from 400 to 1800 cm⁻¹ with a typical acquisition time of 30 sec.

Conclusions

A class of nanohybrids consisting of Ag nanoparticles on both sides of the exfoliated silicate platelets as the support has been developed for the new generation of SERS platform for enhancing the sensitivity of microorganism detection. In contrast to the conventional 2D hot-junctions of traditional “fixed” SERS substrate, the newly developed (3D-hot junctions) SERS substrate provides offered the enhancement of SERS intensity and detection sensitivity. The observed enhancement is explained by the existence of three dimensional (3D) hot junctions, particularly in z-direction of 1-5 nm inter-particle gap distances, displaying ~7 times increase compared to 2D hot-junctions of traditional “fixed” SERS substrate. The SERS substrate in the exfoliated single silicate platelet (Ag/NSP in 3D hot-junctions) exhibited few times higher than that in un-exfoliated multilayered silicate stack (MMT) in the small molecules (adenine) and bacteria (SA) test. The SERS spectra fingerprint of adenine corresponds to bacteria. Therefore, we suppose SERS signal should come from the small molecules released from bacteria.

In addition, the flexible and transparent characteristics (less background interference) of the Ag/NSP SERS substrate could be further modified by the hydrophobic effect of surfactants. It displays about 13 times SERS enhancement in hydrophobic bacteria (i.e., *E. coli*) after modified by surfactant (Ag/NSS), owing to the affinity increase between SERS substrate and the cell wall of bacteria. The uses of 3D hot-junctions of Ag/NSP and surfactant-modified Ag/NSS biochips have broadened the applications for bio-sensing for variety of microorganisms such as irregular-shaped microorganisms (fungi), super hydrophobic bacteria (mycobacteria) (Fig. 7) and larger biological cells (cancer cells), whose are otherwise difficult to be sensitized by 2D hot-junctions of SERS biochips. These findings have advanced SERS technology for possible creation of SERS-based biochips for rapid label-free and cultured-free detections in the various microorganisms from clinical patients.

Acknowledgements

This work was financially supported by National Science Council of Taiwan, the Ministry of Economics of Taiwan, and the Investigator Award of Academia Sinica. We thank Dr. Chin-Ching Lin and Dr. Hung-Chou Liao in Industrial Technology Research Institute (ITRI) for suggestions and Yu-An Su for the cross-section of TEM images by the microtome. Technical supports the Core Facilities for Nanoscience and Nanotechnology at Academia Sinica of Taiwan are acknowledged.

Notes and References

¹Institute of Polymer Science and Engineering, National Taiwan University, Taipei 10617, Taiwan

²Department of Materials Engineering, Ming Chi University of Technology, New Taipei City 24301, Taiwan

³Institute of Atomic and Molecular Sciences, Academia Sinica, Taipei 10617, Taiwan

⁴Research Program on Nanoscience and Nanotechnology, Academia Sinica, Taipei 11529, Taiwan

⁵Institute of Physics, Academia Sinica, Taipei 11529, Taiwan

⁶Center for Condensed Matter Sciences, National Taiwan University, Taipei 10617, Taiwan

⁷Department of Physics, National Taiwan University, Taipei 10617, Taiwan

Corresponding Author(s): T. Y. Liu (* email: tyliu0322@gmail.com) and J. J. Lin (** email: jianglin@ntu.edu.tw)

References

- [1] M. Aizawa, J. M. Buriak, *Chem. Mater.*, 2007, **19**, 5090.
- [2] J. Chen, B. Wiley, J. McLellan, Y. Xiong, Z. Y. Li, Y. Xia, *Nano Lett.* **2005**, 5, 2058.
- [3] T. Sun, K. Seff, *Chem. Rev.*, 1994, **94**, 857.
- [4] S. M. Magaña, P. Quintana, D. H. Aguilar, J. A. Toledo, C. Ángeles-Chávez, M. A. Cortés, L. León, Y. Freile-Pelegrián, T. López, R. M. Torres Sánchez, *J. Mol. Catal. A Chem.*, 2008, **281**, 192.
- [5] H. L. Su, C. C. Chou, D. J. Hung, S. H. Lin, I.C. Pao, J. H. Lin, F. L. Huang, R. X. Dong, J. J. Lin, *Biomaterials*, 2009, **30**, 5979.
- [6] H. L. Su, S. H. Lin, J. C. Wei, I. C. Pao, S. H. Chiao, C. C. Huang, S. Z. Lin, J. J. Lin,

- PLoS ONE*, 2011, **6**, e21125
- [7] J. J. Lin, W. C. Lin, R. X. Dong, S. H. Hsu, *Nanotechnology*, 2012, **23**, 065102.
- [8] R. A. Tripp, R. A. Dluhy, Y. Zhao, *Nano Today*, 2008, **3**, 31.
- [9] B. D. Moore, L. Stevenson, A. Watt, S. Flitsch, N. J. Turner, C. Cassidy, D. Graham, *Nat. Biotechnol.*, 2004, **22**, 1133.
- [10] C. M. Shachaf, S. V. Elchuri, A. L. Koh, J. Zhu, L. N. Nguyen, D. J. Mitchell, J. Zhang, K. B. Swartz, L. Sun, S. Chan, R. Sinclair, G. P. Nolan, *PLoS One*, 2009, **4**, e5206.
- [11] X. Qian, X. H. Peng, D. O. Ansari, Q. Yin-Goen, G. Z. Chen, D. M. Shin, L. Yang, A. N. Young, M. D. Wang, S. Nie, *Nat. Biotechnol.*, 2008, **26**, 83.
- [12] R. M. Jarvis, R. Goodacre, *Chem. Soc. Rev.*, 2008, **37**, 931.
- [13] H. H. Wang, C. Y. Liu, S. B. Wu, N. W. Liu, C. Y. Peng, T. H. Chan, C. F. Hsu, J. K. Wang, Y. L. Wang, *Adv. Mater.*, 2006, **18**, 491.
- [14] T. T. Liu, Y. H. Lin, C. S. Hung, T. J. Liu, Y. Chen, Y. C. Huang, T. H. Tsai, H. H. Wang, D. W. Wang, J. K. Wang, Y. L. Wang, C. H. Lin, *PLoS One*, 2009, **4**, e5470.
- [15] T. Y. Liu, K. T. Tsai, H. H. Wang, Y. Chen, Y. H. Chen, Y. C. Chao, H. H. Chang, C. H. Lin, J. K. Wang, and Y. L. Wang, *Nat. Commun.*, 2011, **2**, 538.
- [16] T. Y. Liu, Y. Chen, H. H. Wang, Y. L. Huang, Y. C. Chao, K. T. Tsai, W. C. Cheng, C. Y. Chuang, Y. H. Tsai, C. Y. Huang, D. W. Wang, C. H. Lin, J. K. Wang, and Y. L. Wang, *J. Nanosci. Nanotechnol.*, 2012, **12**, 5004.
- [17] R. S. Sinha, M. Okamoto, *Prog. Polym. Sci.*, 2003, **28**, 1539.
- [18] N. Aihara, K. Torigoe, K. Esumi, *Langmuir*, 1998, **14**, 4945.
- [19] N. Kakuta, N. Goto, H. Ohkita, T. Mizushima, *J. Phys. Chem. B*, 1999, **103**, 5917.
- [20] K. Shimizu, S. Komai, T. Kojima, S. Satokawa, A. Satsuma, *J. Phys. Chem. C*, 2007, **111**, 3480.
- [21] K. Shimizu, A. Satsuma, *Appl. Catal. B*, 2007, **77**, 202.
- [22] J. Liu, J. B. Lee, D. H. Kim, Y. Kim, *Colloids Surf. A*, 2007, **302**, 276.
- [23] J. Shibata, K. Shimizu, Y. Takada, A. Shichi, H. Yoshida, S. Satokawa, Atsushi Satsuma, T. Hattori, *J. Catal.*, 2004, **227**, 367.
- [24] J. J. Lin, C. C. Chu, C. C. Chou, F. S. Shieu, *Adv. Mater.*, 2005, **17**, 301.
- [25] J. J. Lin, C. C. Chu, M. L. Chiang, W. C. Tsai, *J. Phys. Chem. B*, 2006, **110**, 18115.
- [26] S. Nie, S. R. Emery, *Science*, 1997, **275**, 1102.
- [27] Y. Fang, N. H. Seong, D. D. Dlott, *Science*, 2008, **321**, 388.
- [28] J. Huang, L. Zhang, B. Chen, N. Ji, F. Chen, Y. Zhang, Z. Zhang, *Nanoscale*, 2010, **2**, 2733.
- [29] X. Zhang, M. A. Young, O. Lyandres, R. P. Van Duyne, *J. Am. Chem. Soc.*, 2005, **127**, 4484.
- [30] Y. Han, Z. Liang, H. Sun, H. Xiao, H. L. Tsai, *Appl. Phys. A*, 2011, **102**, 415.
- [31] K. Xu, J. Huang, Z. Ye, Y. Ying, Y. Li, *Sensors*, 2009, **9**, 5534.
- [32] K. Kneipp, A. S. Haka, H. Kneipp, K. Badizadegan, N. Yoshizawa, C. Boone, K. E. Shafer-Peltier, J. T. Motz, R. R. Dasari, and M. S. Feld, *Appl. Spectrosc.*, 2002, **56**, 150.
- [33] A. Sujith, T. Itoh, H. Abe, K. Yoshida, M. S. Kiran, V. Biju, M. Ishikawa, *Anal. Bioanal. Chem.*, 2009, **394**, 1803.
- [34] F. J. García-Vidal, J. B. Pendry, *Phys. Rev. Lett.*, 1996, **77**, 1163.
- [35] L. Gunnarsson, E. J. Bjerneld, H. Xu, S. Petronis, B. Kasemo, M. Kall, *Appl. Phys. Lett.*, 2001, **78**, 802.
- [36] Y. Lu, G. L. Liu, L. P. Lee, *Nano Lett.*, 2005, **5**, 5.

- [37] A. Wei, B. Kim, B. Sadtler, S. L. Tripp, *Chem. Phys. Chem.*, 2001, **2**, 743.
- [38] M. Xu, M. J. Dignam, *J. Chem. Phys.*, 1994, **100**, 197.
- [39] C. C. Chou, J. J. Lin, *Macromolecules*, 2005, **38**, 230.

Figure Caption

Figure 1. Schematic illustration of the Ag nanohybrids consisting of Ag nanoparticles on nano-silicate platelets (Ag/NSP). **(a)** Preparation of Ag/NSP. **(b)** Preparation of surfactant-modified Ag/NSP (Ag/NSS). **(c-g)** TEM images of various Ag/NSP weight ratio of compositions: **(c)** Ag1/NSP99, **(d)** Ag7/NSP93, **(e)** Ag15/NSP15, **(f)** Ag30/NSP70, **(g)** Ag50/NSP50 (scale bar: 25 nm)

Figure 2. 3-dimensional hot-junctions of Ag/NSP SERS substrate and interaction with bacteria **(a)** Schematic showing 3D hot-junctions (particularly in z-direction) of Ag/NSP SERS substrate; inter-particle gap in z-direction is about 1-5 nm and in x-y directions is about 5-50 nm. **(b)** Top view of TEM image showing silver nanoparticles adsorbed on the both sides of NSP (darker ones: top side; grayer ones: bottom side, scale bar: 20 nm). **(c)** Cross section of TEM image showing NSP in a dimension of approximately $100 \times 100 \times 1 \text{ nm}^3$, and indicating silver nanoparticles adsorbed on the both sides of NSP (scale bar: 50 nm). **(d)** Schematic illustration of Ag/NSP SERS substrate interacting with bacteria, derived from the observations of adhesion and entanglement phenomena taken by SEM of **(e)** *S. aureus* (SA) and **(f)** *E. coli* (EC) interactions. (scale bar: $1 \mu\text{m}$)

Figure 3. Relationship between SERS intensity and inter-particle gap of Ag nanoparticles from bacteria. **(a)** SERS spectra of *S. aureus* (SA) measured by various Ag/NSP weight ratio of SERS substrate. **(b)** Integrated Raman intensity (I_{Stokes} is the average Raman signal per Ag particle) of SA between 700 and 770 cm^{-1} as a function of the inter-particle gap (W) for different Ag/NSP ratio substrates (un-exfoliated montmorillonite, MMT, thickness: $\sim 20 \text{ nm}$ as the reference); The normalized SERS intensity ($I_{\text{Stokes}}/I_{\text{Stokes}}^{\infty}$ ratio) as a function of the W/D ratio for different Ag/ASP ratio substrates in the inset figure ($I_{\text{Stokes}}^{\infty}$ is SERS intensity for the largest inter-particle gap, Ag 1/NSP 99, $\sim 50 \text{ nm}$; D is the particle diameter measured by TEM).

Figure 4. Relationship between SERS intensity and inter-particle gap of Ag nanoparticles from small molecules. **(a)** SERS spectra of small molecules (adenine from DNA) measured by various Ag/NSP weight ratio of SERS substrate. **(b)** Integrated Raman intensity of adenine between 700 and 770 cm^{-1} as a function of the inter-particle gap (W) for different Ag/NSP ratio substrates (un-exfoliated MMT as the reference); The normalized SERS intensity ($I_{\text{Stokes}}/I_{\text{Stokes}}^{\infty}$ ratio) as a function of the W/D ratio for different Ag/ASP ratio substrates in the inset figure

Figure 5. Relationship between inter-particle gap in z-direction (W_z) and absorption wavelength of Ag/NSP nano-hybrid substrate.

Figure 6. Differentiation of SERS intensity between Ag/NSP and the surfactant-modified Ag/NSP (Ag/NSS) as SERS substrates for detection of different bacteria. SERS spectra of *S. aureus* (SA, hydrophilic bacteria) and *E. coli* (EC, hydrophobic bacteria) on Ag/NSP versus Ag/NSS SERS substrate.

Figure 7. SERS spectra of mycobacteria (super-hydrophobic bacteria) and fungi (irregular-shaped and larger microorganisms) using Ag/NSS SERS substrate.

Figure 1

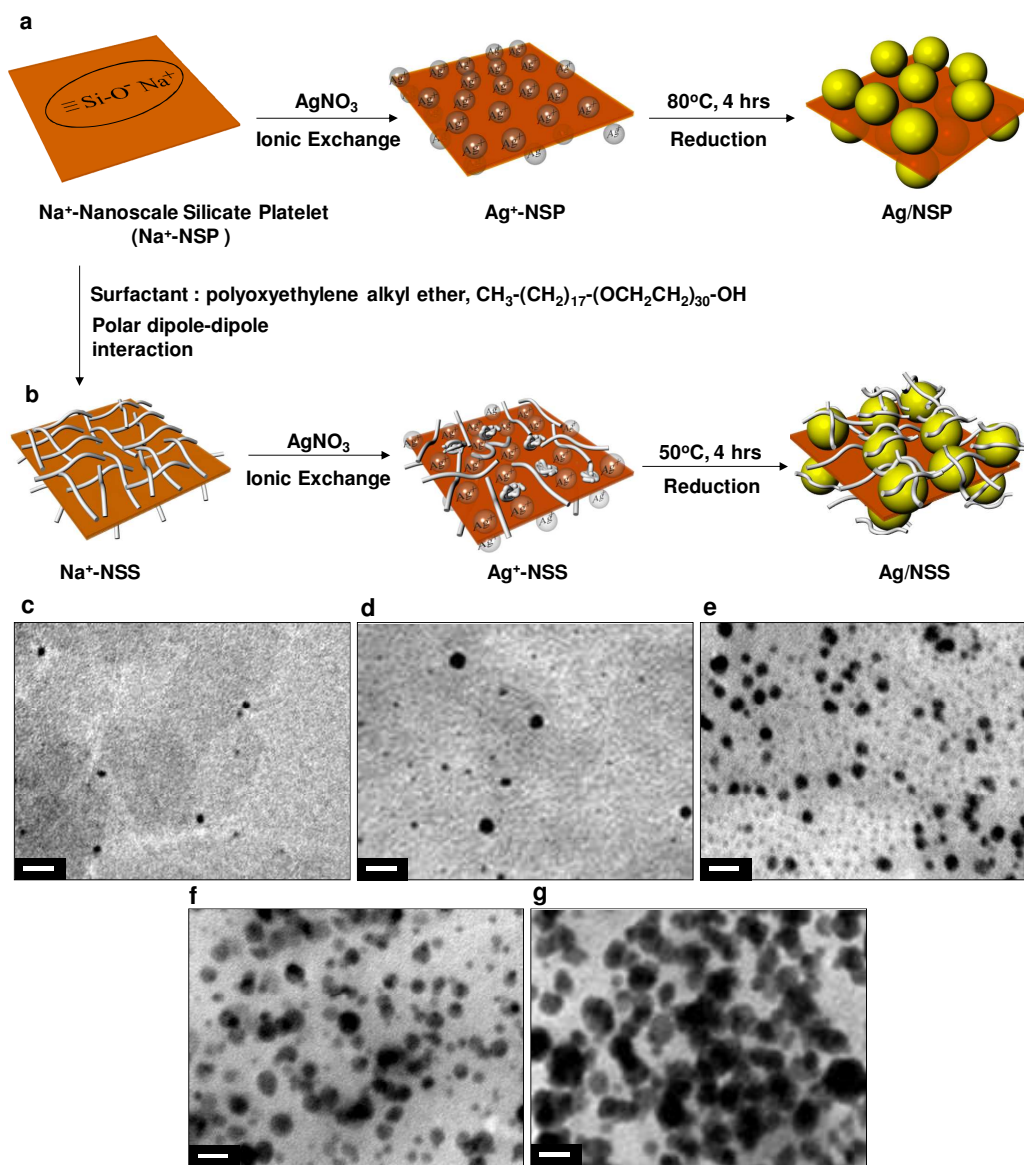


Figure 2

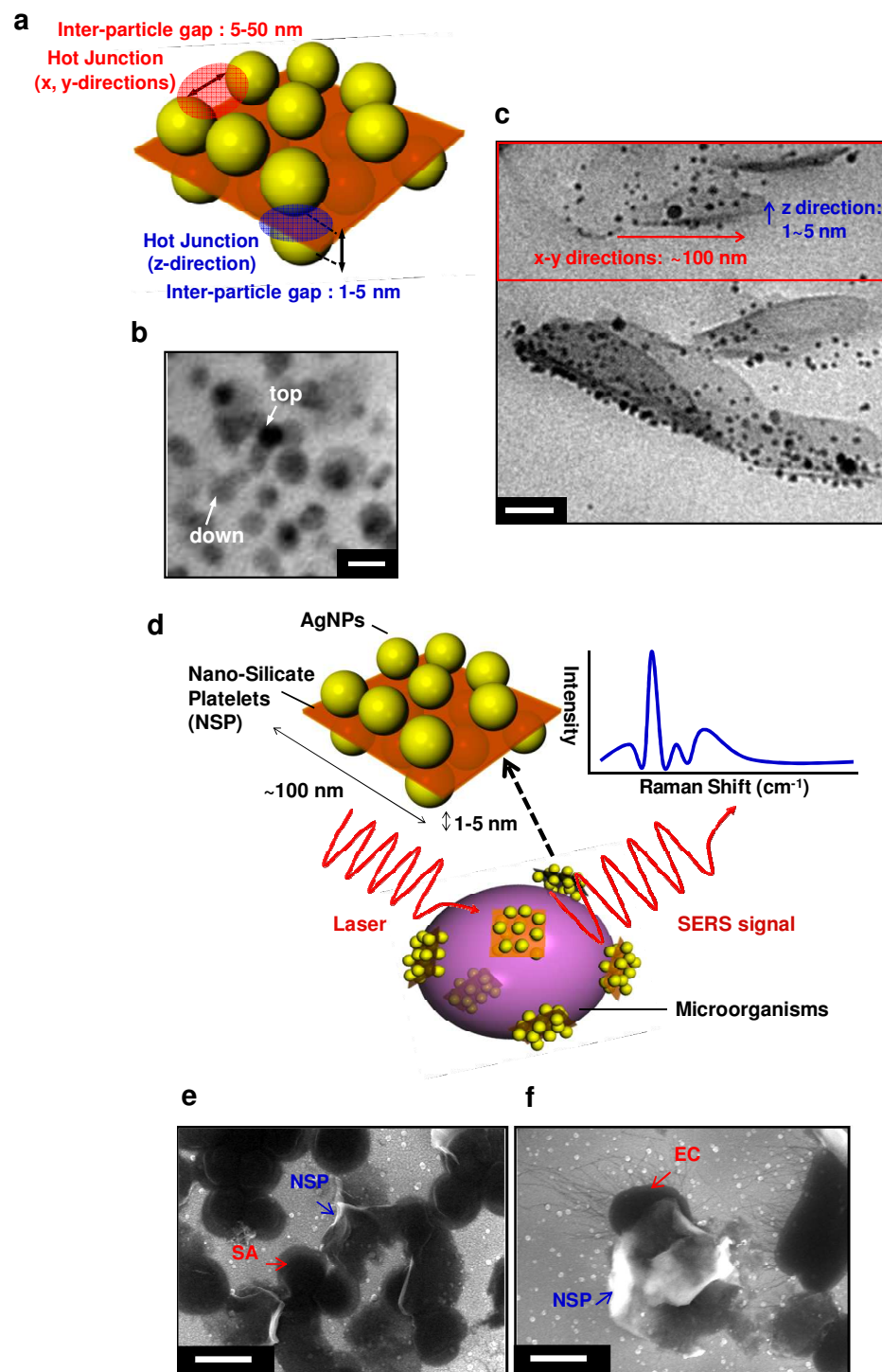


Figure 3

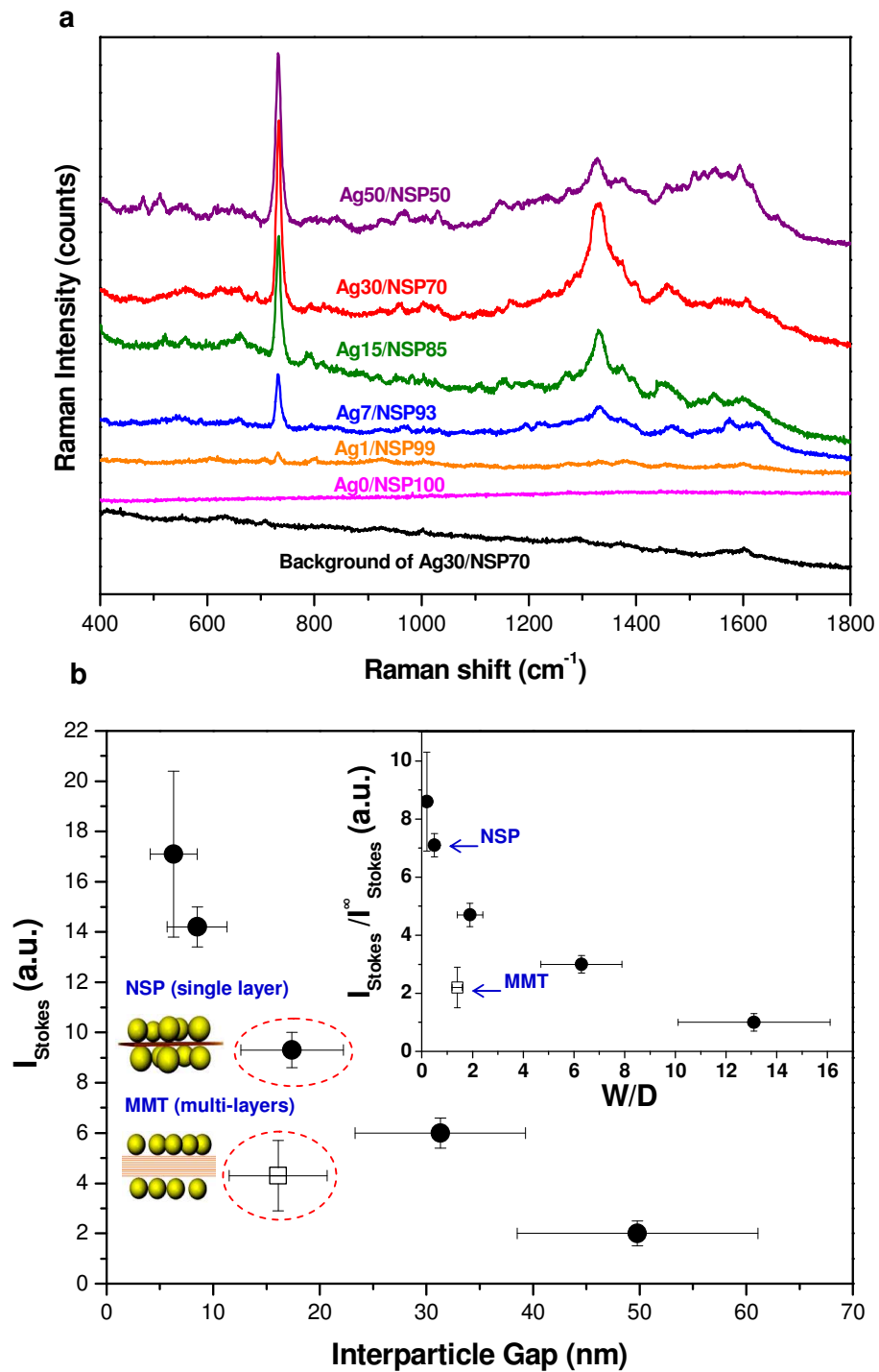


Figure 4

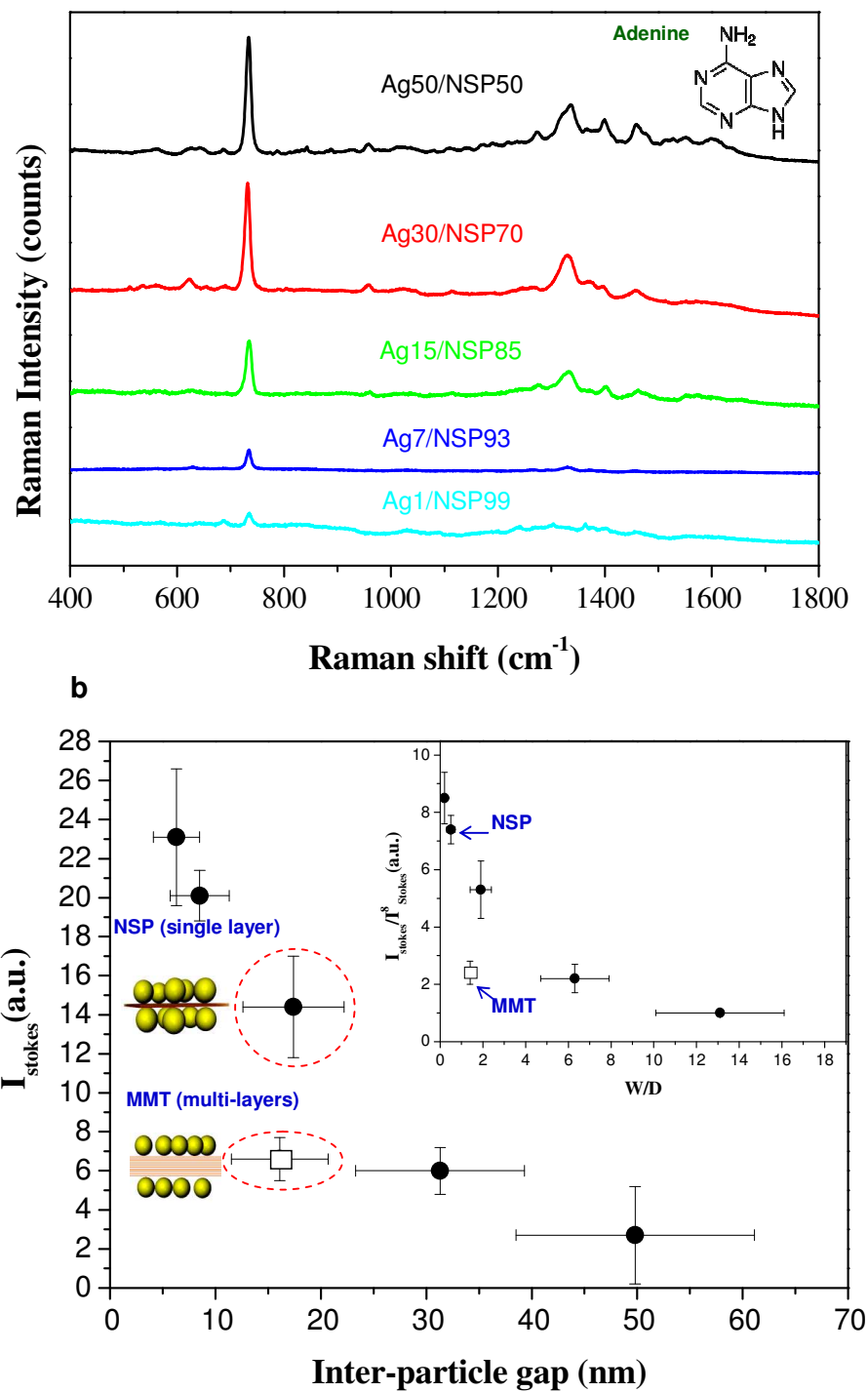


Figure 5

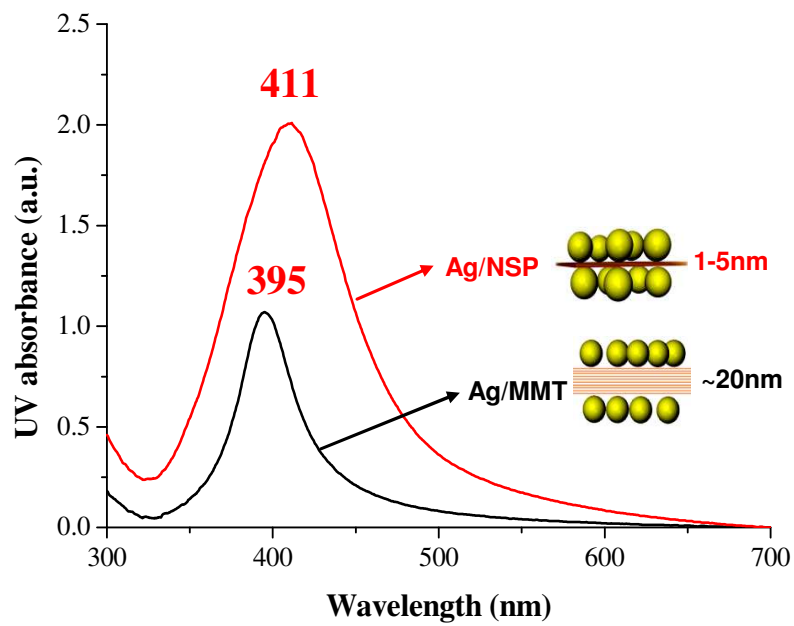


Figure 6

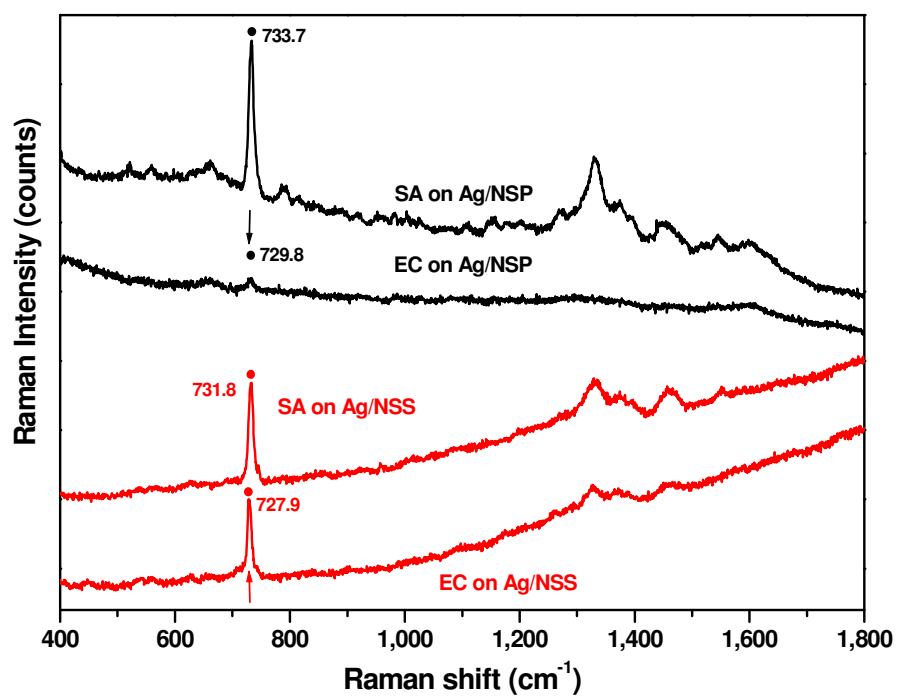


Figure 7

